heritage

MDPI

Article

On Devotional Artworks: A Non-Invasive Characterization of Pigments of the *Madonna della Croce* Wall Painting in Triggiano (Bari, Southern Italy)

Giovanna Fioretti [1,*], Cinzia Campobasso [2], Giacomo Eramo [1], Alessandro Monno [1] and Gioacchino Tempesta [1]

[1] Earth and Geoenvironmental Science Department, University of Bari Aldo Moro, 70125 Bari, Italy
[2] Pasquale Battista Foundation, 20121 Milano, Italy
* Correspondence: giovanna.fioretti@uniba.it

Abstract: Devotional artworks represent a valuable form of art, as they are evidence of religious worship and the demo-ethno-anthropological, as well as historical-artistic, heritage of a community, which is why they definitely belong to the cultural identity of a geographic area. The *Madonna della Croce* wall painting is an example of devotional art preserved today in the homonymous church in Triggiano (Bari, Italy). The presented study concerns the characterization of pigments used in the painting. The identification of pictorial materials had the aim of providing a contribution to knowledge about the painting, the history of restorations, and other historical events, and to increase the information about the Apulian painting to better reconstruct the social, cultural, and economic contexts of the region. Through a non-invasive and fast methodological approach, including portable digital microscopy, colorimetry, fibre optic reflectance spectroscopy (FORS), and X-ray fluorescence spectroscopy (XRF); 42 points considered on coloured areas were analysed in situ, and results on pigment identification were achieved. According to the local wall painting tradition, red and yellow ochres, green earth, vine black, massicot, and lead-tin yellow were found. Furthermore, both indigo-woad dye and a mixture of vine black and yellow ochre to obtain a blueish colour on the Virgin's mantle were highlighted.

Keywords: painting; devotional artworks; conservation; pigments; FORS; XRF; colorimetry; portable microscopy

Citation: Fioretti, G.; Campobasso, C.; Eramo, G.; Monno, A.; Tempesta, G. On Devotional Artworks: A Non-Invasive Characterization of Pigments of the *Madonna della Croce* Wall Painting in Triggiano (Bari, Southern Italy). *Heritage* **2023**, *6*, 4263–4281. https://doi.org/10.3390/heritage6050225

Academic Editors: Manuela Vagnini, Chiara Anselmi and Francesca Volpi

Received: 19 April 2023
Revised: 8 May 2023
Accepted: 9 May 2023
Published: 11 May 2023

1. Introduction

The *Madonna della Croce* portrait is painted on a lunette, previously detached from a wall of unknown origin and now preserved on the right of the main altar in the *Madonna della Croce* church in Triggiano (Bari, Italy). The wall painting depicts the Virgin and Child with St. Sebastiano and St. Rocco with their symbols of martyrium and was realised by a local artist who worked between 1550 and 1570 in the town. The numerous legends about the wall painting, mixed with documented historical events, talk about miraculous healing stories that strengthened the strong relationship of the Triggiano inhabitants with this religious symbol. In fact, the painting immediately became a precious worship artwork, so much so that a church was built and dedicated to this Virgin, chosen as the main saint of the town [1].

The veneration of painted fragments, accidentally found and portraying the Virgin with Child, is quite recurrent in the region. Although they usually show poor quality and were made by unknown artists, these artworks acquire an inestimable value for the faithful due to their miraculous power. For such reasons, they feed the pilgrimage flows and certainly belong to the local cultural heritage.

Similarly to the *Madonna della Croce* case, some valuable regional examples of the phenomenon are the *Madonna del Pozzo* church in Capurso [2], the *Madonna della Scala* church in Massafra (Taranto) [3], and the *Madonna di Pozzo Faceto* shrine in Fasano (Brindisi) [4].

Recently, a renewed cultural interest in the *Madonna della Croce* church and its famous painting occurred, thanks to a conservation and valorisation project of the whole cultural heritage of Triggiano designed and promoted by local institutions and organisations. The results of these studies were published in some scientific papers [5,6] and in a volume [7].

Moreover, other research is moving forward, and specific papers are upcoming, in particular on the church Baroque altars, following the photogrammetric method for the marble mapping [8,9].

The paper, concerning the characterization of painting pigments and their mixtures used in the pictorial layers, is part of the abovementioned project for the conservation, promotion, and enhancement of the cultural heritage of Triggiano. It has the purpose of contributing to the very scarce current knowledge about it in terms of used materials and the history of restorations. Secondly, the presented research contributes to increasing knowledge of the Apulian painting and to better reconstructing the social, cultural, and economic contexts of the region.

The *Madonna della Croce* portrait depicts the Virgin and Child with St. Sebastiano and St. Rocco with their symbols of martyrium and shows the Apulian traditional colour palette marked by the use of red, yellow, green, and grey pigments, very frequent in rupestrian paintings [10–13] and also in churches and in other archaeological contexts [5,14–18]. However, in the regional artistic production, the limited number of pigments was offset with a mix of two or more pigments to guarantee colour variability. This custom has a very interesting technical value as it has the purpose, on the one hand, to emulate much more expensive pigments, including, for example, lapis lazuli and cinnabar, and on the other hand, to enrich the artist's palette with a higher number of nuances and shades.

For the characterization of pigments in surface pictorial layers, in addition to the most common investigation techniques, including Raman spectroscopy and X-ray fluorescence spectroscopy, the current literature also provides numerous examples of the effectiveness of fibre optic reflectance spectroscopy [19–23], colorimetry [24–26] and portable digital microscopy [27–29].

These methods are portable and non-invasive and have the advantage of being quick and rather economical (in comparison with other traditional techniques), as well as providing immediate results. Limitations to consider are the effects of some factors, above all the heterogeneity of pictorial surfaces and pigments, the presence of surface alterations due to natural ageing or pollution, and the addition of protective or restoration products to the painting. Such aspects could lead to a misinterpretation of the analytical result. Clearly, to minimise identification errors, it is essential that the results obtained from each of these techniques are not individually studied and interpreted but compared. Generally, a winning strategy to overcome this limit could be the selection of complementary analytical techniques, as presented in the paper. Furthermore, the preliminary observation of the painting by digital optical microscopy allows prior evaluation of aspects related to the heterogeneity (natural or anthropic) of the pictorial surfaces.

An efficient approach based on the matching of results obtained by means of portable microscopy, FORS, and colorimetry for the identification of pigments and their mixtures in wall painting was proposed by Fioretti et al. [29]. This multianalytical approach, which also provides a detailed library of results and photomicrographs, was considered for the analysis of pictorial material in the *Madonna della Croce* painting, and the obtained results were compared with XRF data.

The Painting

The painting (Figure 1) is composed of three parts: the central one, showing the Virgin enthroned with the Child, is wider than the other two, which display the depiction of St. Rocco on the right and St. Sebastiano on the left. The Virgin is seated on a throne, which

can almost be glimpsed due to the presence of the lateral armrests placed at her sides. She has a red tunic and a blueish grey mantle with a yellow border that creates a cut in the composition of the painting. Her halo is yellow. The Child, wrapped on his mother's left arm, wears a yellow tunic and the typical Christ's cruciferous nimbus, showing intense red and yellow colours. In his left hand, three yellow flowers are painted. The skin of the Virgin and the Child is yellow, and their dresses show black decoration patterns.

Figure 1. Measuring points of the *Madonna della Croce* painting (Triggiano, Southern Italy).

The two martyr saints are depicted with the symbols of their sacrifice: St. Sebastiano is illustrated during the arrow torture, tied to a yellow tree trunk. St. Rocco shows his typical pilgrim's clothes, a wound on the right thigh, a symbol of the plague, and other traditional iconographic features. The faces and hands of these figures are coloured with a very pale colour. The background behind the saints is white and decorated with flowers.

2. Analysis Points

Since the methodological approach was completely non-invasive, sampling was not necessary, and the investigations were conducted directly in situ. On the painting, 9 red, 9 fleshy pink, 11 yellow, 4 green, 5 blueish grey, and 4 black points were considered for a total of 42 analysis points. The considered red points were part of the Madonna's tunic (R4, R5), St. Sebastiano's mantle, the Child's halo, the flowers, and the background. Yellow points were measured on the trunk and the arrows, on the halos of the Virgin, the Child, and the two saints, on the Child's tunic, on the Virgin's mantle, and on a flower. Referring to the green areas, three points were selected in correspondence to the tunic of St. Rocco and the background behind the Virgin. On the mantle of the Virgin were selected all the blueish-grey points. The selected black points were on the rim and decoration of the Virgin and St. Rocco's mantles, on an arrow piercing St. Sebastiano, and on St. Rocco's boot. Finally, a fleshy colour was evaluated on the yellow-pink areas of the Virgin's and Child's

face and hand and on the pale-yellow points of St. Sebastiano's face and hand. A mapping of the measuring points was shown in Figure 1 and reported in Table 1.

Table 1. Sample names, grouped by colour, corresponding areas on the painting, and analysis methods (DM—digital microscope; SPC—spectrophotocolorimetry) carried out.

Colour	Sample	Area	Analysis Methods
Red	R1	Child's halo	DM, SPC, FORS
	R2	Child's halo	DM, SPC, FORS, XRF
	R3	Child's halo	DM, SPC, FORS, XRF
	R4	Virgin's tunic	DM, SPC, FORS, XRF
	R5	Virgin's tunic	DM, SPC, FORS
	R6	Flower	DM, SPC, FORS
	R7	Flower	DM, SPC, FORS
	R8	St. Vito's mantle	DM, SPC, FORS, XRF
	R9	Background	DM, SPC, FORS, XRF
Yellow	Y1	Tree trunk (St. Sebastiano)	DM, SPC, FORS
	Y2	Tree branch (St. Sebastiano)	DM, SPC, FORS, XRF
	Y3	St. Sebastiano's halo	DM, SPC, FORS
	Y4	Child's halo	DM, SPC, FORS
	Y5	Virgin's halo	DM, SPC, FORS
	Y6	Rim of Virgin's mantle	DM, SPC, FORS, XRF
	Y7	St.Vito's halo	DM, SPC, FORS
	Y8	Child's tunic	DM, SPC, FORS
	Y9	Rim of Virgin's mantle	DM, SPC, FORS
	Y10	Flower	DM, SPC, FORS, XRF
	Y11	Rim of Virgin's mantle	DM, SPC, FORS, XRF
Fleshy Pink	S1	St. Sebastiano's face	DM, SPC, FORS, XRF
	S2	Child's face	DM, SPC, FORS, XRF
	S3	Virgin's face	DM, SPC, FORS, XRF
	S4	St. Vito's face	DM, SPC, FORS
	S5	Virgin's hand	DM, SPC, FORS, XRF
	S6	Child's hand	DM, SPC, FORS, XRF
	S7	Virgin's hand	DM, SPC, FORS
	S8	St. Vito's hand	DM, SPC, FORS
Green	G1	St. Vito's tunic	DM, SPC, FORS, XRF
	G2	Background	DM, SPC, FORS, XRF
	G3	Background	DM, SPC, FORS
	G4	Background	DM, SPC, FORS
Grey/blue	B1	Virgin's mantle	DM, SPC, FORS
	B2	Virgin's mantle	DM, SPC, FORS
	B3	Virgin's mantle	DM, SPC, FORS, XRF
	B4	Virgin's veil	DM, SPC, FORS
	B5	Virgin's mantle	DM, SPC, FORS, XRF
Black	B6	Neck of St. Vito's mantle	DM, SPC, FORS, XRF
	B7	Decoration of Virgin's mantle	DM, SPC, FORS
	B8	Rim of Virgin's mantle	DM, SPC, FORS
	B9	Decoration of Virgin's mantle	DM, SPC, FORS, XRF
	B10	Arrow (St. Sebastiano)	DM, SPC, FORS
	B11	St. Vito's boot	DM, SPC, FORS, XRF

3. Methods

The preparation layer without painting and all the considered 42 points (which will be called "samples" for convenience, even if they were not physically detached from the pictorial surface) were analysed by portable digital microscopy, FORS, and colorimetry. In order to avoid repetition and promote a sustainable research approach, an efficient strategy for the XRF analysis was designed starting from the obtained results in terms of microscopic description, colorimetric coordinate values, and reflectance spectra of pigments. Then, the

chemical composition of 21 samples and the preparation layer was evaluated by XRF. In Table 1, the considered analytical techniques were reported for each sample.

3.1. Optical Microscopy

The microscopic observation of painted surfaces was carried out by a Dino-Lite Edge Digital Microscope AM7915MZT, equipped with an automatic magnification reading (10–220×), a light polarizer, and a 5-megapixel resolution sensor; 8 switchable LEDs with an infrared filter (>650 nm) constitute the illumination system. The microscope is portable and handy thanks to its length of 10 cm. It allows for focused photomicrographs by means of an extended depth of field and an extended dynamic range system.

For the microscopic characterization of samples, the observation of peculiar markers proposed by Fioretti et al. [29] was followed. It considered the chromatic, morphological, optical, and other features of pigment particles and their relationship with the background. Specifically, they were texture (unimodal or multimodal), observing the degree of sorting [30], size, colour (hue, saturation, brightness), shape, rounding (rounded, mixed, angular), gloss (high, medium, low), edge (sharp, thick, soft), and appearance (intact, mixed, fractured).

3.2. Colorimetry

For the measurement of the colorimetric coordinates, a Konica Minolta CM-2600d portable spectrophotocolorimeter was used. Experimental conditions were: D65 standard illuminant, aperture mask with a diameter of 6 mm, standard observer at a 10° angle, wavelength range from 360 to 740 nm with a wavelength step size of 10 nm. The instrument was calibrated using zero and white calibration provided by the instrument producer. The device, set for the CIEL*a*b* system [31], acquired the three values of L* (brightness), a* (green-red axis), and b* (blue-yellow axis) three times, which were post-processed to obtain the main value and standard deviation.

3.3. Fiber Optic Reflectance Spectroscopy

FORS analysis was performed by means of a custom system by Avantes. The AvaSpec-ULS2048XL-USB2 model spectrophotometer and an AvaLight-HAL-S tungsten halogen light source were combined with the reflection probe FCR-7UV200-2-ME UV/VIS. The spectrophotometer's spectral resolution was about 1.4 nm, and the wavelength range was from 200 to 1100 nm. Spectra were recorded from 300 to 900 nm because of noise in the UV and IR regions. The probe had a diameter of about 200 µm. A WS-2 reference tile was used to standardise the diffuse reflectance spectra of samples. The spot size was about 2 mm in diameter, and the distance between probe and sample was about 5 mm. The instrument setting was as follows: 400 ms integration time, 10 scans, for a total acquisition time of 4 s for each spectrum. The spectra were collected with Avasoft 8.0 and then exported in Spectragryph® (version v1.2.16) [32] for visualisation and comparison with standards.

3.4. XRF

Twenty-one points were analysed in situ by means of a custom portable XRF instrument. The X-ray source was a Mini-X with an Au target operating at 40 kV and 95 µA by AMPTEK Inc., Bedford, MA, USA. The detector was a silicon drift (SDD) XR-123 SDD with a 25 mm^2 detection area, 500 µm thickness (fully depleted), and a 12.5 µm Be window by AMPTEK Inc., Bedford, MA, USA. The resolution at 5.9 keV was 135 eV at room temperature. The system had a fixed geometry; the X-ray beam is at a 90° angle with the detector. This geometry allowed partially polarised radiation with a high background reduction in Compton scattering. Samples were analysed directly in the air at room temperature. The outgoing radiation was collimated into a 5 mm beam diameter at the sample surface. Each acquisition had a fixed working distance (15 mm) between the instrument and the painting surface, controlled by a laser interferometer. The acquisition time for each spectrum was 60 s. Spectra for qualitative analyses were elaborated with the software

Spectragryph® [32]. Generally, XRF analysis performed in the air generates some physical limits for lighter element detection. In our case, with the previously described setup, only elements with Z equal to or higher than 16 (S) were detectable. Low traces of Fe, Ni, Cu, and Zn that belonged to the instrument components (slit and case) could be present in the acquired spectra.

4. Results

4.1. Microscopic Characterisation

The observation by the portable digital microscope allowed us to evaluate the parameters observed as key markers by Fioretti et al. [29] for all 42 samples and to suppose the nature of pigments on the basis of comparison with their data. Thanks to these observations, samples with similar characteristics were grouped. The results were reported in detail in Table 2 and illustrated below.

Almost all the dark red samples (R1, R2, R3, R4, R5, R6, R7, and R8) showed remarkable homogeneity, given by an opaque red pigment with an average size of about 25 μm, massive shape, and sharp edge, to which a moderate amount of black pigment was added, with an average size of 25 μm, tabular shape, and angular rounding (Figure 2a). The red colour of the background was due to the finer fraction of the red pigment, which was invisible to the microscope magnification (lower than 220×). The parameters observed on both pigments would seem to be consistent with red ochre [24,29,33,34] and vine black (C) [29,35] markers, respectively. The most common red ochres used as pigment in the wall paintings are those composed of earth deposits rich in Fe(III) oxides, and the main chromophore is hematite (Fe_2O_3) [34]. An exception was represented by sample R9 (Figure 2b), which showed a pale red shade due to an extremely fine pigment that was not visible at the instrument magnification. The black pigment recognised in the first group of reds was missing in the second one.

The yellow samples were grouped into two types. The first (Figure 2c) belonged golden yellow samples (Y1, Y2, Y3, Y4, Y5, Y6, Y7, Y8, and Y10), which were characterised by a yellow and a black pigment. The first, showing bimodal texture, was composed of a fine fraction not visible under the microscope, which determined the colour of the background, and opaque yellow pigment particles with a size of about 30 μm, massive and rounded shape, and a sharp edge. The black pigment showed a mean size of 20 μm, a tabular shape, and angular rounding. These parameters were very similar to those of yellow ochre [24,29,33,34] and vine black, respectively. Similarly to red ochre, generally, yellow ochre is an earth deposit rich in Fe(III) oxides, where colour is due to α-FeOOH (goethite) and rarely γ-FeOOH (lepidocrocite) [34]. The second group of yellow (Figure 2d) included samples Y9 and Y11. They showed a dark yellow colour given by an extremely fine pigment (<10 μm) with massive form. In this case, the microscopic features were well-matched with those of massicot (PbO) [29,36].

Samples considered on the figure's skin were divided into two groups on the basis of their microscopic key markers. The first group (Figure 2e) included samples S2, S3, S5, S6, and S7, in which the surface pictorial layer consisted of a pigment made up of dark yellow spherical particles (about 70 μm). In this case, the pigment could not be identified under the optical microscope because it did not display significant key features. Occasionally, the presence of an extremely fine pinkish colour, composed of rare pink particles smaller than 10 μm, was also distinguished. The second group includes samples S1, S4, and S8, where a black pigment with an average size of 15 μm and a tabular and angular rounding shape was identifiable as vine black.

Table 2. Summary of observation by digital portable microscope, reporting distinctive parameters of each pigment. (*—naked-eye colour; n.v.—not visible; n.i.—not identifiable).

Colour	Sample	Attribution	Texture	D Moda	Colour							Morphology				
					Unpolarised Light				Polarised Light							
					Hue	Saturation	Brightness	Gloss	Hue	Saturation	Brightness	Gloss	Shape	Rounding	Edge	Appearance
Dark red	R1, R2, R3, R4, R5, R6, R7, R8	Red ochre	bimodal	25 µm	red	medium-low	low	low	red	medium-low	low	low	massive	rounded	sharp	intact
				n.v.	red	medium-low	low	n.v.	red	medium-low	low	n.v.	n.v.	n.v.	n.v.	n.v.
		Vine black	unimodal	25 µm	black	medium	medium-high	high	black	low	low	low	tabular	angular	soft	intact
Pale red	R9	n.i.	unimodal	n.v.	orange	low	low	n.v.	orange	low	low	n.v.	n.v.	n.v.	n.v.	n.v.
Gold yellow	Y1, Y2, Y3, Y4, Y5, Y6, Y7, Y8,	Yellow ochre	bimodal	n.v.	yellow	low	low	n.v.	yellow	low	low	n.v.	n.v.	n.v.	n.v.	n.v.
				30 µm	yellow	low	low	low	yellow	low	low	low	massive	rounded	sharp	intact
		Vine black	unimodal	20 µm	black	medium	medium-high	high	black	low	low	low	tabular	angular	soft	intact
Dark Yellow	Y9, Y10, Y11	Massicot	unimodal	<10 µm	yellow	high	high	medium	yellow	high	high	medium	massive	mixed	soft	intact
Yellow	S2, S3, S5, S6, S7	n.i.	unimodal	70 µm	brown	medium	low	low	brown	medium	low	low	n.v.	n.v.	n.v.	n.v.
		n.i.	unimodal	n.v.	pink	low	low	n.v.	pink	low	low	n.v.	n.v.	n.v.	n.v.	n.v.
		Vine black	unimodal	20 µm	black	medium	medium-high	high	black	low	low	low	tabular	angular	soft	intact
Pale yellow	S1, S4, S8	Vine black	unimodal	15 µm	black	medium	medium-high	high	black	low	low	low	tabular	angular	soft	intact
Green	G1, G2, G	Green earth	bimodal	n.v.	green	low	medium	n.v.	green	low	low	n.v.	n.v.	n.v.	n.v.	n.v.
				40 µm	green	low	low	low	green	medium	medium	medium	massive	rounded	sharp	intact
		Yellow ochre	unimodal	30 µm	yellow	low	low	low	yellow	medium	medium	low	massive	rounded	sharp	intact
		Hematite	unimodal	100 µm	red	high	high	high	high	high	high	high	massive	rounded	sharp	intact
		Vine black	unimodal	40 µm	black	medium	medium-high	high	black	low	low	low	tabular	angular	soft	intact
Pale green	G4	n.i.	unimodal	n.v.	green	low	low	n.v.	green	low	low	n.v.	n.v.	n.v.	n.v.	n.v.
Grey	B1, B2, B3	Vine black	unimodal	15 µm	black	medium	medium-high	high	black	low	low	low	tabular	angular	soft	intact
		Yellow ochre	unimodal	30 µm	yellow	low	low	low	yellow	low	low	low	massive	rounded	sharp	intact
Grey-blue	B4, B5	Vine black	unimodal	25 µm	black	medium	medium-high	high	black	low	low	low	tabular	angular	soft	intact
		n.i.	unimodal	n.v.	blue	medium	low	low	blue	medium	low	medium	n.v.	n.v.	n.v.	n.v.
Black	B6, B7, B8, B9, B10, B11	Vine black	unimodal	30 µm	black	medium	medium-high	high	black	low	low	low	tabular	angular	soft	intact

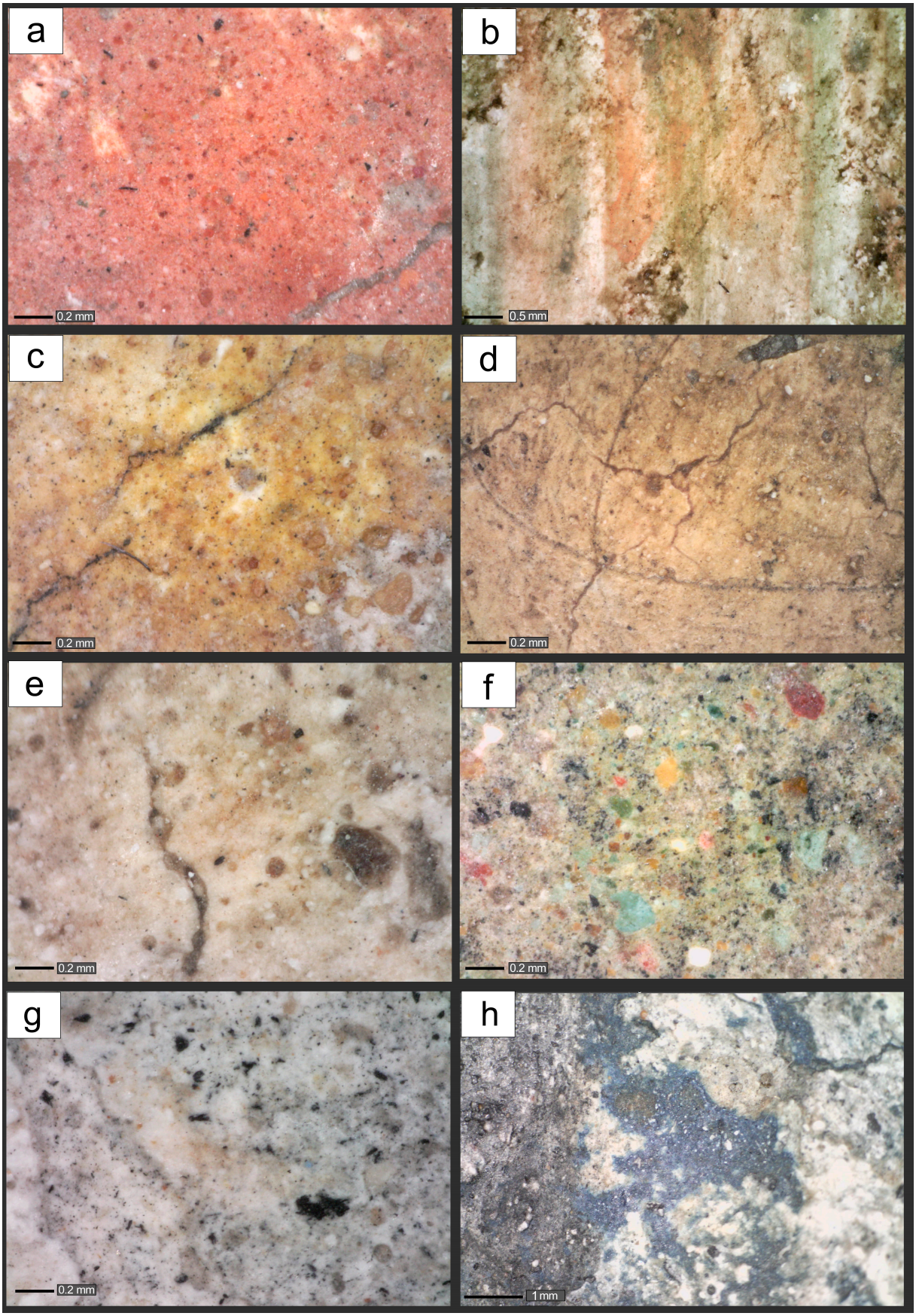

Figure 2. Photomicrographs of samples R5 (**a**), R9 (**b**), Y2 (**c**), Y9 (**d**), S2 (**e**), G1 (**f**), S2 (**g**), and B4 (**h**).

The green samples were distributed into two types based on their microscopic key markers. The first type (Figure 2f) included samples G1, G2, and G3, which were characterised by the presence of 4 different pigments, consisting of: green particles marked by bimodal distribution due to an invisible very fine fraction and a coarser portion (40 μm) composed of green, massive, and rounded particles with a sharp edge; particles of a yellow pigment of about 30 μm, characterized by a massive and angular shape and sharp edges; red particles, whose size fluctuated between 20 and 100 μm and colour was a very saturated and bright red; black particles, showing a mean size of 25 μm, tabular shape, and angular rounding. These pigments could refer to green earth [29,37], yellow ochre, red ochre, pure hematite, and vine black, respectively. Green earths are also coloured by Fe, which is included in the constituting clay minerals (i.e., celadonite and glauconite) [38]. The second type (Figure 2b) exclusively consisted of sample G4, which displayed a very transparent green coloration whose pigment was not visible under the microscope.

As regards the grey and blue samples, the microscopic observations allowed for the identification of two chromatic groups. The first (Figure 2g), including samples B1, B2, and B3, revealed the presence of black and fine (15 μm) particles of pigment, marked by a tabular shape, referable to the vine black. In addition, rare particles of yellow ochre were recognised. The second group (Figure 2h), on the other hand, was made up of samples B4 and B5 and differed from the first in the presence of a blue colour, turning green at some point, in which the pigment particles could not be recognised.

Finally, the black samples (B6, B7, B8, B9, B10, and B11) were found to be composed of black and fine (10 μm) pigment particles, marked by tabular shape and identifiable as vine black.

4.2. Colorimetry

Spectrophotocolorimetry provided L*a*b* colorimetric coordinates for each sample, reported in Table 3, even if the a* and b* coordinates, plotted in the biplot in Figure 3a, provided more meaningful indications.

In red pigments, b* values were centred between 12.3 and 20.2, whereas a* values were more scattered and covered a range from 9 to 24.9. Except for sample R9, all the other reds appeared strongly correlated (R^2 = 0.95), as shown in the biplot reported in Figure 3b.

Yellow pigments were arranged in a plot area with a* and b* values between 8.6 and 16.1 and between 20.3 and 35.4, respectively. However, a bimodal distribution of points was observed, as samples Y1, Y3, Y7, Y9, Y10, and Y11 differed for lower values of a* and

Similarly, points corresponding to the flashy pink of the painting seemed to be separated into two rather distinct groups, in which the first one was made up of samples S1, S4, and S8 and was characterised by lower a* and b* values, while the second one appeared more scattered towards higher values of a* and b* and included samples S2, S3, S5, and S6. For sample S7, the colorimetric coordinates indicated an intermediate position with respect to the two previous clusters. The a* and b* values for skin samples ranged from 3.7 to 8.2 and 12.3 to 22.8, respectively.

In the 4 green samples, a* and b* values oscillated between 1.1 and 2.9 and between 14.9 and 19.5, respectively. The grey points were rather spread out along the b* axis, where values ranged from 4.9 to 11.5, and more centred along the a* axis, where values ranged from −0.2 to 2.2.

Finally, the values of a* and b* in the black samples appeared concentrated between 0 and 1, with slightly negative values, and between 1 and 5.3, respectively.

Table 3. L*, a*, and b* mean values and standard deviation of each point.

Colour	Sample	L*	L* st. Dev.	a*	a* st. Dev.	b*	b* st. Dev.
Red	R1	41.111	0.317	20.185	0.316	17.467	0.245
	R2	43.300	0.174	20.510	0.067	18.996	0.084
	R3	39.455	0.341	19.757	0.167	17.119	0.230
	R4	40.224	0.271	24.914	0.162	20.233	0.217
	R5	43.237	0.301	21.100	0.149	18.041	0.206
	R6	40.938	0.208	18.445	0.184	16.138	0.127
	R7	38.921	0.179	13.640	0.154	12.286	0.081
	R8	46.902	0.253	16.431	0.147	14.261	0.119
	R9	55.585	0.107	9.016	0.037	15.787	0.010
Yellow	Y1	55.472	0.190	8.652	0.153	20.371	0.134
	Y2	51.056	0.100	13.086	0.063	27.622	0.025
	Y3	58.849	0.217	8.666	0.175	22.412	0.018
	Y4	54.662	0.231	11.587	0.151	27.215	0.148
	Y5	59.172	0.147	16.153	0.051	35.371	0.143
	Y6	51.434	0.227	15.663	0.073	31.756	0.274
	Y7	58.589	0.239	9.646	0.185	20.954	0.064
	Y8	58.240	0.189	11.909	0.052	30.956	0.139
	Y9	62.909	0.277	8.700	0.201	23.240	0.132
	Y10	51.473	0.117	8.647	0.025	21.981	0.012
	Y11	62.487	0.127	8.754	0.024	23.890	0.285
Fleshy pink	S1	77.013	0.196	3.725	0.050	15.876	0.020
	S2	61.776	0.194	6.991	0.056	19.109	0.061
	S3	62.322	0.143	6.681	0.017	22.512	0.032
	S4	74.226	0.134	3.835	0.088	14.306	0.011
	S5	65.641	0.330	8.237	0.303	22.791	0.098
	S6	62.013	0.191	7.158	0.026	21.194	0.103
	S7	70.405	0.263	4.496	0.169	19.479	0.077
	S8	80.846	0.114	2.998	0.030	12.332	0.004
Green	G1	54.743	0.170	2.929	0.075	17.233	0.054
	G2	44.432	0.272	1.639	0.078	15.822	0.156
	G3	47.157	0.330	1.128	0.058	14.872	0.179
	G4	63.925	0.222	2.744	0.136	19.487	0.118
Blue-grey	B1	62.030	0.247	1.413	0.171	7.675	0.036
	B2	55.858	0.329	1.989	0.242	9.303	0.105
	B3	52.117	0.368	2.226	0.209	11.481	0.145
	B4	42.595	0.158	−0.185	0.093	8.270	0.055
	B5	40.857	0.237	−0.035	0.007	4.880	0.065
Black	B6	44.190	0.117	0.736	0.016	3.420	0.018
	B7	33.855	0.084	−0.002	0.004	3.156	0.035
	B8	30.658	0.454	0.176	0.082	2.733	0.053
	B9	34.367	0.854	1.042	0.151	5.281	0.299
	B10	33.825	0.181	0.333	0.123	2.017	0.038
	B11	33.661	0.179	0.269	0.073	1.042	0.035

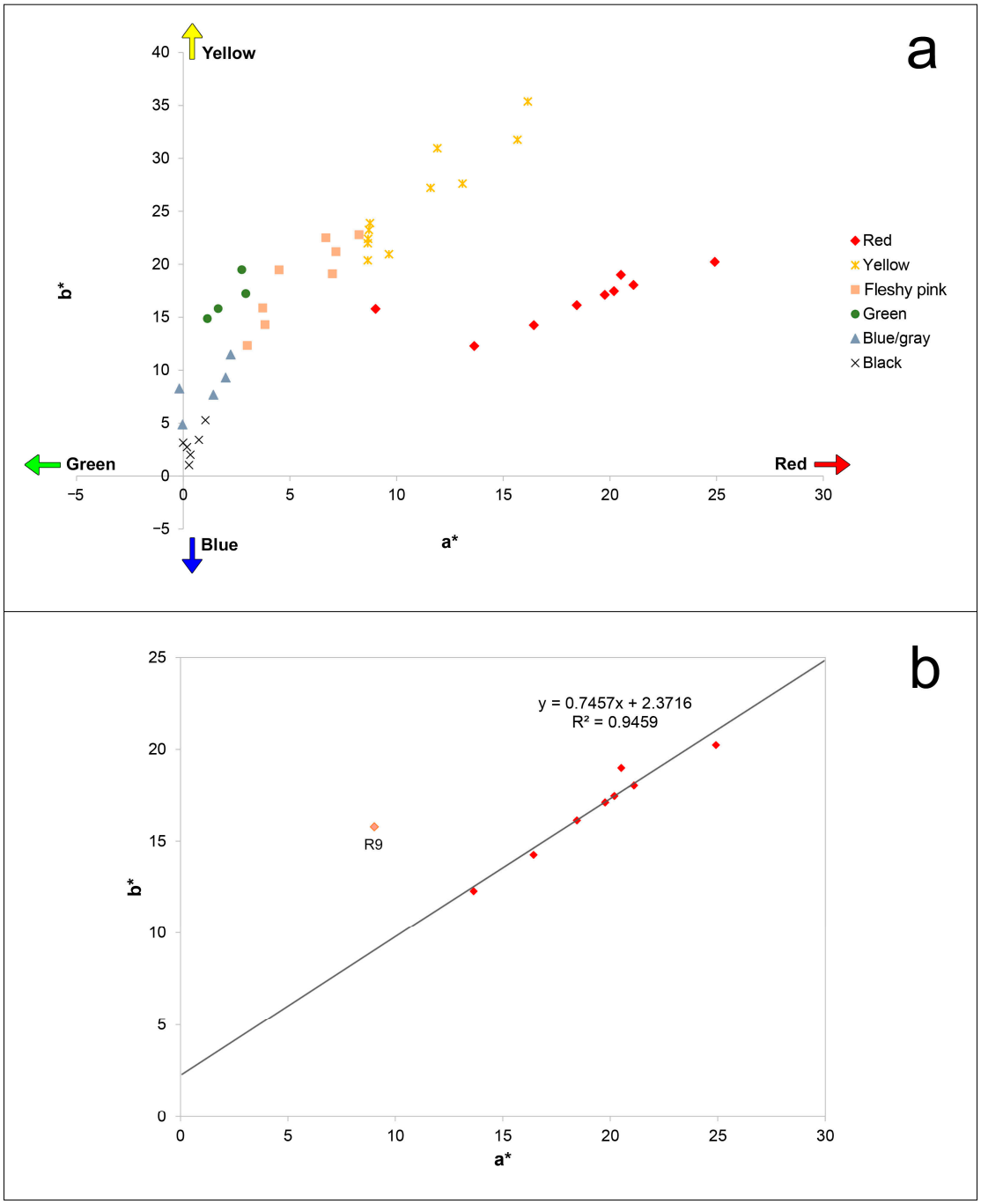

Figure 3. Biplot of a* and b* values of CIEL*a*b* coordinates measured on all the considered points (**a**); biplot of a* and b* values of CIEL*a*b* coordinates measured in red areas, showing the correlation line (**b**).

4.3. FORS

All the samples were analysed by FORS, and the obtained spectral features, shown in Table 4, were compared with the databases and the available literature in order to recognise the pigments inside the surface pictorial layers of the painting. Red samples showed similar reflectance spectra (Figure 4a), characterised by an S shape, a maximum reflectance centred at ~750 nm, and an absorption after about 800 nm, suggesting the presence of red ochre [20,29].

Table 4. FORS spectral features of samples.

Color	Sample	FORS Spectral Features	Attribution	References
Red1	R1, R2, R3, R4, R5, R6, R7, R8, R9	~750 nm (max); absorption after ~800 nm	Red ochre	[20,29]
Yellow 1	Y1, Y2, Y3, Y4, Y5, Y6, Y7, Y8,	~770 nm (max)	Yellow ochre	[20,29]
Yellow 2	Y9, Y10, Y11	~525 nm (i.p.)	Yellow ochre + massicot or lead-tin yellow	[20,29]
Fleshy pink 1	S2, S3, S5, S6, S7	~770 nm (max)	Yellow ochre	[20,29]
Fleshy pink 2	S1, S4, S8	flat spectrum	-	-
Green	G1, G2, G3	~570 nm (max); ~750 nm (max)	Green earth + yellow ochre	[20,29,39]
Grey 1	B1, B2, B3	flat spectrum	-	-
Grey 2	B4, B5	600–800 nm (absorption band)	Indigo dye	[40,41]
Black	B6, B7, B8, B9, B10, B11	flat spectrum	-	-

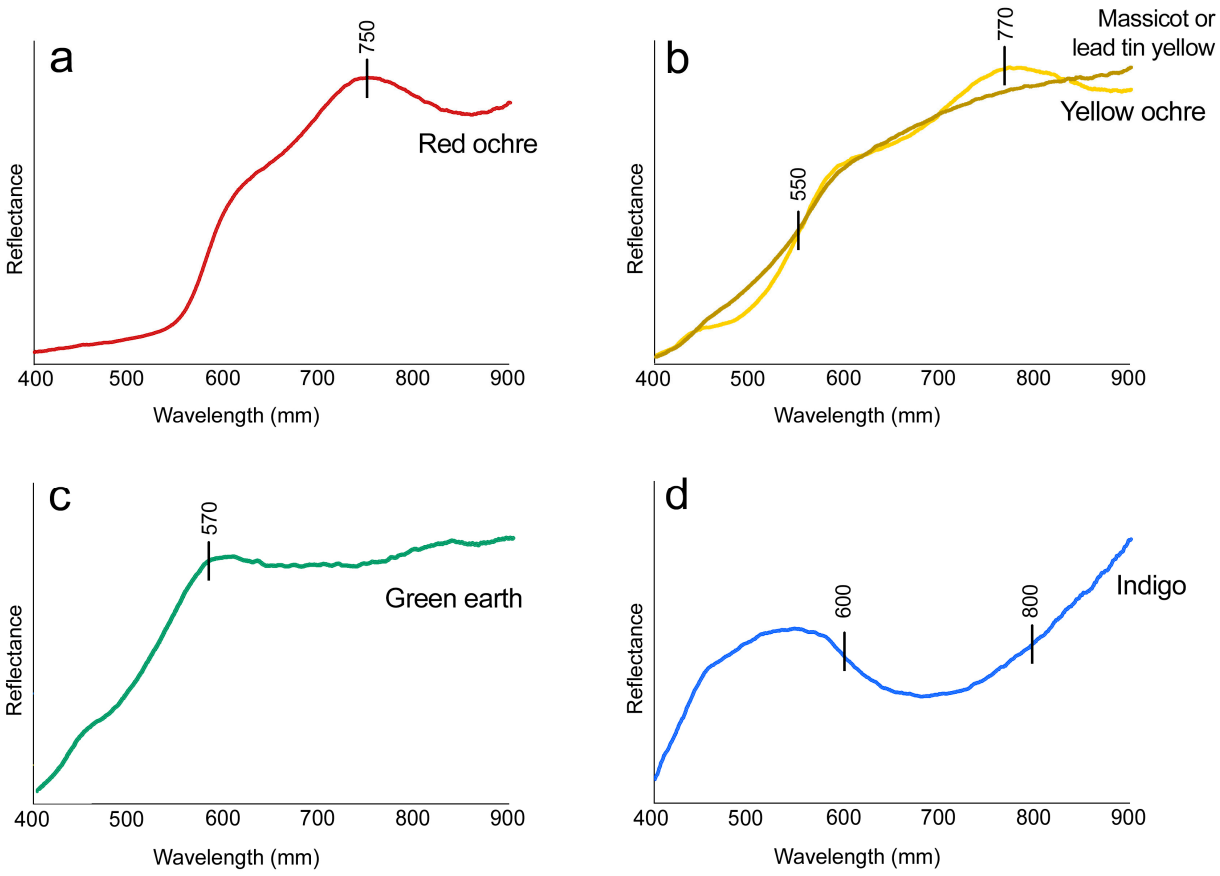

Figure 4. Representative FORS reflectance spectra for the red (**a**), yellow (**b**), green (**c**), and blue (**d**) areas of the painting.

As for the yellow samples (Figure 4b), the spectral fingerprints suggested clustering. In fact, the spectra of samples Y2, Y4, Y5, Y6, and Y8 were characterised by an S-shape and a maximum reflectance at ~770 nm, which are spectral characteristics of yellow ochre [20,29]. Samples Y9, Y10, and Y11 had a reflectance curve slightly comparable with that of yellow ochre and showed an inflection point at ~560 nm referable to both massicot and lead-tin

yellow. In this case, FORS results should suggest the presence of a mixed composition of yellow ochre and massicot, or lead-tin yellow, in the sample [20,29].

Regarding the skin areas of the figures in the painting, the FORS results highlighted the existence of two groups. The first one included samples S2, S3, S5, S6, and S7, whose spectra revealed a maximum of reflectance centred at ~770 nm, referable to the yellow ochre [20,29]. Differently, samples S1, S4, and S8 of the second group showed almost flat spectra without fingerprints.

FORS spectra (Figure 4c) of green areas revealed reflectance maxima centred at ~570 nm, referable to green earth [20,29,39], and ~750 nm, ascribable to yellow ochre [20,29].

In grey and black samples, the FORS spectra appeared flat and featureless; however, in samples B4 (Figure 4d) and B5, they revealed two reflectance bands centred at ~450 nm and ~550, attributable to blue and green colour contributions, respectively, and an absorption band between 600 and 800 nm. Although the curve was strongly flattened by the black pigment contribution, it was comparable with that of organic dyes such as indigo or woad [40,41], even if chemical elemental analysis is more useful for identification.

4.4. XRF

The XRF analyses were performed on all the pigments recognised on the wall paintings by means of microscopy, spectrocolorimetry, and FORS. Each spectrum revealed the main elements that confirmed the pigment identified by FORS or excluded mineral pigments in the case of organic ones. Traces of Pb in the background spectrum and in almost all the spectra acquired on painted areas were referable to the preparation layer, except for black samples B6, B7, and B11, where the painting was very dense and opaque and the contribution of the preparation layer was irrelevant. The presence of Pb could indicate the use of *biacca* ($2PbCO_3 \cdot Pb(OH)_2$). Other low traces of Ni, Cu, and Zn belonged to the instrument component.

In order to achieve a complete identification of mineral pigments, it was necessary to consider the amount of each element acquired.

For the red areas (R2, R3, R4, R8, and R9), spectra revealed the presence of high amounts of Fe, Ca, K, and Ti. Such elements should be related to red ochre, which generally, together with the chromophore iron oxides, contains additional phases such as anatase (TiO_2) and other minerals [33]. In Figure 5a, the spectrum of the R8 sample was reported, which clearly represented the composition of the pigment used in all the red areas.

Referring to the yellow areas, XRF spectra confirmed the presence of high amounts of Pb, Fe, and Sn in sample Y11, which suggested the use of a mix composed of massicot, yellow ochre, and a lower amount of lead-tin yellow. Ca and Fe were probably connected to the substrate. The Pb counts were lower in samples Y2 and Y6, where the identified peaks were those related to Fe, suggesting the presence of yellow ochre. Figure 5b,c showed the yellow ochre and mix of massicot, yellow ochre, and lead-tin yellow, respectively.

The spectra of flashy areas showed two cases: in the first, including samples S2, S3, S5, and S6, the presence of a moderate amount of Fe, Ca, and K suggested the presence of impure yellow ochre, whereas in the second case (sample S1), the result excluded the presence of the pigment.

The analyses of green parts (G1, G2) highlighted the presence of Fe and, in addition, K, Ca, and Ti as proof of the presence of a common impure green earth [33]. The XRF spectrum of a representative green was reported in Figure 5d.

For blue areas (B5), the spectrum did not show characteristic peaks of mineral pigments, so results suggested excluding mineral pigments such as azurite, commonly used for blue paintings, and hypothesising the use of an organic blue, i.e., woad or indigo [42]. A summary of XRF results is reported in Table 5.

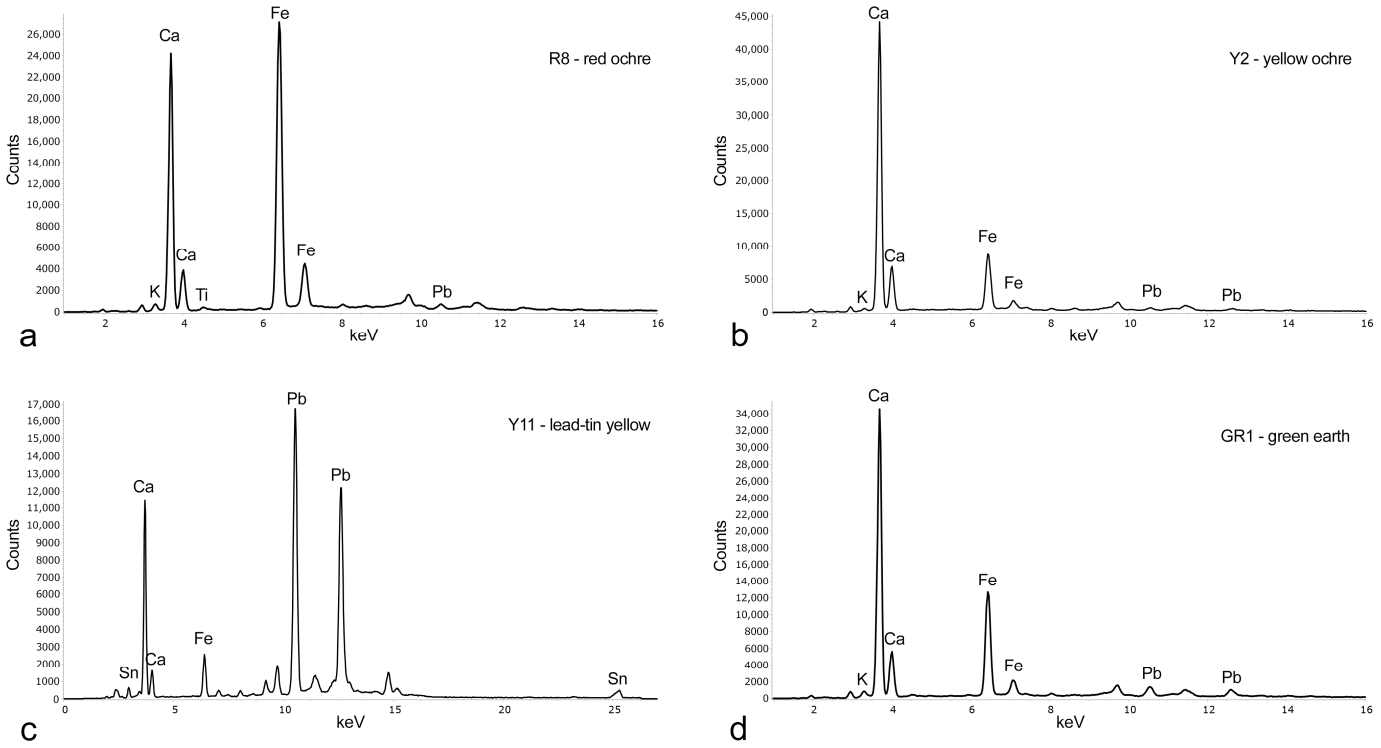

Figure 5. Representative XRF spectra for red ochre (**a**), yellow ochre (**b**), a mix of massicot, yellow ochre and lead-tin yellow (**c**), and green earth (**d**).

Table 5. Summary of XRF results. (+—major elements; −—minor elements; tr—traces).

Colour	Sample	XRF	Attribution
Red	R2, R3, R4, R8, R9	Ca (+), Fe (+), K (tr), Ti (tr), Pb (tr)	Red ochre
Yellow 1	Y2, Y6, Y10	Ca (+), Fe (−), K (tr), Ti (tr), Pb (tr)	Yellow ochre
Yellow 2	Y11	Pb (+), Ca (+), Sn (−), Fe (−), K (tr), Ti (tr)	Massicot + yellow ochre + lead tin yellow
Fleshy pink 1	S2, S3, S5, S6	Ca (+), Fe (−), K (tr), Pb (tr)	Yellow ochre
Fleshy pink 2	S1	Ca (+), Fe (tr), K (tr), Pb (tr)	no mineral pigment identified
Green	G1, G2	Ca (+), Fe (−), K (tr), Ti (tr), Pb (tr)	Green earth
Grey 1	B3	Ca (+), Fe (tr), K (tr), Pb (tr)	no mineral pigment identified
Grey 2	B5	Ca (+), Fe (tr), K (tr), Pb (tr)	no mineral pigment identified
Black	B6, B9, B11	Ca (+), Fe (tr), K (tr)	no mineral pigment identified

5. Discussion

The comparison of microscopic characteristics, colorimetric coordinates measured by spectrophotocolorimetry, and XRF and FORS results made it possible, above all, to identify of the chromatic palette used by the artist. In accordance with the local pictorial

tradition [5,10–18], the use of common pigments, in particular ochres and earths, and their mixtures were observed.

Obtained data highlighted a homogeneity of red pictorial layers measured on the Virgin's and Child's halos, on the Virgin's tunic, on St. Rocco's mantle, and on flowers. An exception was represented by sample R9, measured in the background behind the Virgin and Child figures, which, although having the same reflectance spectrum and the same chemical composition obtained by FORS and XRF, respectively, showed different microscopic features, in particular in the texture and grain size. In fact, microscopic observation of the sample and its surrounding area highlighted the presence of an alternating red and green pattern (Figure 2b), attributable to the *tratteggio* integration technique [used during past events of painting conservation and restoration. Additionally, the a* and b* coordinates were not correlated with the other red samples (Figure 3b). Although the pictorial layer included red ochre, as also highlighted by FORS and XRF data, the colorimetric coordinates would confirm that the pigment had different chromatic peculiarities and that, therefore, in agreement with the microscopic observations, it was applied at a different moment.

Referring to the yellow points, yellow ochre (Figures 2c, 4b and 5b) was identified in correspondence with the halos of the Virgin and Child, on the rope of St. Sebastiano, and on some parts of the edge of the Virgin's mantle. Instead of some points corresponding to other areas of the edge of the Virgin's mantle and flowers, XRF results (Figure 5b) resolved all the doubts in the interpretation of FORS spectral features (Figure 4b), confirming the use of a mix composed of massicot, yellow ochre, and lead-tin yellow.

As also demonstrated by the colorimetric coordinates (Figure 3a), on the edge of the Virgin's mantle and on the St. Sebastiano ropes, two shades of yellow (one based on ochre and one based on massicot, yellow ochre, and lead-tin yellow) were placed side by side in an attempt to provide greater realism to the painting.

The flesh tones on the faces and hands of the Virgin and Child were obtained through the use of a very dark yellow ochre, as visible under the microscope (Figure 2e) and demonstrated by FORS and XRF results. Instead, on the faces and hands of the two saints (S1, S4, and S8), the colour was mainly given by the whitish colour of the background; the FORS spectrum did not show spectral features, and the XRF results excluded the presence of a pigment. This aspect was also visible in the point distribution in the a* vs. b* biplot (Figure 3a). The distinction between two types of flesh tone could possibly suggest the hypothesis of a retouching of the flesh tones on the faces and hands of the Virgin and Child. The use of yellow ochre for the fleshy paint is an element rarely found in local wall paintings, where the pictorial tradition considers the use of red ochre, possibly mixed with white pigment or lime, for the incarnates [5,11]. Even in this case, the yellow ochre would seem to be applied without the addition of a white pigment (or at most mixed with lime) but directly on the plaster, exploiting its natural light colour.

Partially confirmed by XRF (Figure 5c) and FORS (Figure 4c) spectra, the microscopic observations (Figure 2f) of the green areas in correspondence to the background and to St. Rocco's tunic revealed the presence of a more complex mixture of pigments, consisting of green earth, yellow ochre, and red ochre. The latter was not detected in the FORS spectrum due to its overlapping with yellow ochre. Furthermore, points corresponding to the green samples in the biplot in Figure 3 were not positioned in the 2nd quarter as expected but moved to higher values of a* and b* in the 1st quarter. This shift would suggest a significant content of yellow and subordinately red components.

The results of the microscopic observations (Figure 2g) of the grey points highlighted the presence of carbon black and rare particles of yellow ochre on the grey areas of the Virgin's tunic on the bottom and on the left side. In fact, according to literature [5,11,13], a blueish tone is reachable from the mixing of these two pigments.

However, in correspondence to the veil and the right side of the Virgin's mantle, a blue component, together with the previous black pigment, was clearly visible under the microscope (Figure 2h). The microscopic observation highlighted a homogeneous and compact pictorial layer, above all devoid of markers and features (i.e., texture, gloss)

typical of the most common inorganic blue [29]. In addition, XRF analysis did not detect the presence of chemical elements related to the unknown blue pigments. Conversely, although the FORS spectrum (Figure 4d) was strongly influenced by the black particles, it confirmed the presence of an organic dye, i.e., indigo or woad [40,41]. However, the unique identification of the blue dye will be verified by chemical elemental analysis or other investigation techniques. The presence of this blue compound on the veil and on the mantle of the Virgin leads to rejecting the hypothesis of an alteration product or a restoration material, on the one hand for its position on the painting, and on the other hand for the absence of metallic elements detectable by XRF and restoring traces observable under the digital microscope. Such an aspect, even if previously highlighted in the Apulian wall painting [18], represents an interesting artistic practise for blue pictorial layers where the use of black pigments as a replacement of more precious and valuable blue pigments (i.e., lapis lazuli, azurite) was the predominant custom in the regional artistic tradition. Moreover, the absence of the blue dye on the bottom surface of the painting should be correlated to its high solubility and to the low durability of that area due to the touching acts of pilgrims and faithful.

Finally, the black colours in correspondence to edges and decorations were composed exclusively of a black pigment, presumably vine black, as identified under the microscope.

The microscopic analysis of the painted surfaces, supported by the comparison of a* and b* colorimetric coordinates, allowed to highlight areas integrated by modern techniques (*tratteggio*) of restoration on the background behind the Virgin and Child figures that were not completely visible to the naked eye (Figure 6). This aspect definitely suggested a rather recent restoration event, as this restoration technique was introduced in the 1940s [43]. Further, similar areas were not found in the painting.

Figure 6. A detail of one of the restoration areas (delimited by the red outline) identified in the background behind the Virgin.

6. Conclusions

The presented investigation case demonstrated the effectiveness of the non-invasive approaches adopted, such as portable digital microscopy, colorimetry, FORS, and XRF. It proved to be a complementary analytical technique, thanks to which the presence of

organic and inorganic pigments and the coexistence of different pigments in the same pictorial layer can be evaluated. It should be considered that, similarly to other traditional non-destructive investigation techniques currently used in the cultural heritage field, the presented methodology presents serious limits related to the complexity and heterogeneity of the pictorial surfaces. In this sense, portable microscopy could play a key role since it allows for a preliminary screening useful for assessing the type and number of pigments and retouching present on the more superficial pictorial layer. Findings allowed for important new insights on the *Madonna della Croce* painting, which was a very valuable example of devotional art and an important place of pilgrimage in southern Italy. The identification of pigments, such as red and yellow ochres, green earth, and carbon black, confirmed the prevalent use of common raw materials in devotional paintings as well as in the case of the more well-known wall paintings. Similarly, in the local artistic tradition, the expediency of mixing such pigments in order to simulate the effect of precious and more expensive pigments was confirmed by the addition of yellow ochre and red ochre to green earth in the green areas of the studied painting.

The microscopic observations, compared with the results obtained from colorimetric, FORS, and XRF investigations, made it possible to highlight the areas of *tratteggio* integration and, therefore, a restoration that certainly happened after the 1940s not found in written sources to date.

Furthermore, the discovery of the indigo/woad dye for the Virgin's mantle represents a novelty in the region, as previous research revealed mixes of black, red, and/or yellow pigments to obtain blue. In this sense, an interesting future perspective could be to apply the proposed non-invasive approach also to other mural paintings in the area, as it includes complementary analytical techniques that consent to highlight particular characteristics of the painting by means of portable digital microscopy, for example, the restoration areas, and to identify both pigments by XRF and dyes by spectrophotocolorimetry and FORS.

These thoughts certainly contribute to the still fragmentary knowledge about the local pictorial customs, in particular devotional artworks, which are extremely widespread in the region but have never been studied from an archaeometric point of view.

Above all, the results of the research represent an important preliminary goal useful for planning and implementing the imminent restoration, conservation, and enhancement project of the church, no longer only as an object of local devotion but as a cultural heritage of the community.

Author Contributions: Conceptualization, G.F., C.C., A.M. and G.T.; methodology, G.F.; formal analysis: G.F., A.M. and G.T.; investigation, G.F., A.M. and G.T.; writing—original draft; preparation, G.F., C.C. and G.T.; writing—review and editing, G.F, C.C., G.T. and G.E.; visualization, G.F. and G.T.; supervision, G.F. All authors have read and agreed to the published version of the manuscript.

Funding: The research was financially supported by the Italian Ministry of University and Research (Italy) through the National Operational Program (PON) for Research and Innovation 2014–2020 (Project AIM1815472-Activity 2-Line 1).

Data Availability Statement: Data are contained within the article.

Acknowledgments: The authors would like to thank the Pasquale Battista Foundation for the financial support in the project of valorisation and conservation of the Triggiano cultural heritage and Father Francesco Necchia for his courteousness and availability during the research activities.

Conflicts of Interest: The authors declare no conflict of interest.

References

1. Battista, P. *La Madonna Della Croce in Una "Memoria" Del 1737*; Levante Editori: Bari, Italy, 1984.
2. Campobasso, C.; Di Fronzo, D. *Viaggio Alla Scoperta Del Culto Della Madonna Del Pozzo, Storie, Aneddoti e Fotografie Della Protettrice Della Comunità Dei Pugliesi Nel Mondo*; Edizione Fondazione Pasquale Battista: Bari, Italy, 2021.
3. Caprara, R.; Dell'Aquila, C. *Il Villaggio Rupestre Della Gravina "Madonna Della Scala" a Massafra (Taranto)*; Dellisanti Ed.: Massafra, Italy, 2007.
4. Cirillo, M.T.; Pastore, M. *I Santuari. Guida Agli Itinerari Religiosi Tra Puglia e Basilicata*; Di Marsico Libri: Bari, Italy, 2010.

5. Fioretti, G.; Raneri, S.; Pinto, D.; Mignozzi, M.; Mauro, D. The Archaeological Site of St. Maria Veterana (Triggiano, Southern Italy): Archaeometric Study of the Wall Paintings for the Historical Reconstruction. *J. Archaeol. Sci. Rep.* **2020**, *29*, 102080. [CrossRef]
6. Fioretti, G.; Campobasso, C.; Capotorto, S. Digital Photogrammetry as Tool for Mensiochronological Analysis: The Case of St. Maria Veterana Archaeological Site (Triggiano, Italy). *Digit. Appl. Archaeol. Cult. Herit.* **2020**, *19*, e00158. [CrossRef]
7. Fioretti, G.; Campobasso, C. (Eds.) *TRIVIANUM Ricerca, Tutela e Valorizzazione Del Patrimonio Culturale Di Triggiano*; Edizione Fondazione Pasquale BAttista: Bari, Italy, 2021.
8. Fioretti, G.; Acquafredda, P.; Calò, S.; Cinelli, M.; Germanò, G.; Laera, A.; Moccia, A. Study and Conservation of the St. Nicola's Basilica Mosaics (Bari, Italy) by Photogrammetric Survey: Mapping of Polychrome Marbles, Decorative Patterns and Past Restorations. *Stud. Conserv.* **2020**, *65*, 160–171. [CrossRef]
9. Fioretti, G.; Acciani, A.; Buongiorno, R.; Catella, M.A.; Acquafredda, P. Photogrammetric Survey and 3D Model as Experimental Tool for Mapping of Polychrome Marbles in Artworks: The Case of Two Baroque Altars in Bari (Italy). *J. Archit. Conserv.* **2019**, *25*, 90–103. [CrossRef]
10. Capitanio, D.; Laviano, R.; Menga, A.; Meo-Evoli, N.; Vona, F.; Vurro, F. Intonaci e Pitture Murali dell'ipogeo di san Matteo All'arena, Monopoli (Bari). In *Sulle Pitture Murali*; Arcadia Ricerche: Marghera-Venezia, Italy, 2005; pp. 1137–1146.
11. Pinto, D.; Laviano, R.; Bianchi, V. Archaeometric Investigations on Wall Paintings from the Hypogeum of S. Marco (Fasano—Brindisi, Southern Italy). *Plinius* **2008**, *34*, 348.
12. Calia, A.; Giorgi, M.; Quarta, G.; Masieri, M. Le Pitture Della Cripta Del Gonfalone a Tricase (Lecce): Problematiche Stori-Co-Artistiche e Contributo Alla Identificazione Dei Pigmenti Attraverso FRX Portatile. In Proceedings of the BENI CULTURALI IN PUGLIA Dialoghi Multidisciplinari per la Ricerca, la Tutela e la Valorizzazione, Bari, Italy, 16–17 September 2020; pp. 125–132.
13. Fioretti, G.; Garavelli, A.; Germinario, G.; Pinto, D. Archaeometric Study of Wall Rock Paintings from the Sant'Angelo in Criptis Cave, Santeramo in Colle, Bari: Insights on the Rupestrian Decorative Art in Apulia (Southern Italy). *Archaeol. Anthropol. Sci.* **2021**, *13*, 168. [CrossRef]
14. Calia, A.; Giannotta, M.T. *La Tomba Dei Festoni Di Via Crispi A Taranto: Individuazione E Riconoscimento Dei Pigmenti Utilizzati Nelle Pitture*; D'Amico, C., Ed.; Pàtron Editore: Bologna, Italy, 2005; pp. 271–278.
15. Calia, A.; Melica, D.; Quarta, G. I Dipinti Murali Del Tempietto: Materiali Costituenti e Tecniche Esecutive. In *Masseria Seppannibale Grande in agro di Fasano (BR)*; Bertelli, G., Lepore, G., Eds.; Adda Editore: Bari, Italy, 2011; pp. 195–206.
16. Pinto, D. Analisi di alcuni campioni di intonaco dipinto della cupola orientale. In *Masseria Seppannibale Grande in agro di Fasano (BR)*; Bertelli, G., Lepore, G., Eds.; Adda Editore: Bari, Italy, 2011; pp. 207–209.
17. De Benedetto, G.E.; Fico, D.; Margapoti, E.; Pennetta, A.; Cassiano, A.; Minerva, B. The Study of the Mural Painting in the 12th Century Monastery of Santa Maria Delle Cerrate (Puglia-Italy): Characterization of Materials and Techniques Used: Study of Painting at the Santa Maria Delle Cerrate Church. *J. Raman Spectrosc.* **2013**, *44*, 899–904. [CrossRef]
18. Fico, D.; Pennetta, A.; Rella, G.; Savino, A.; Terlizzi, V.; De Benedetto, G.E. A Combined Analytical Approach Applied to Medieval Wall Paintings from Puglia (Italy): The Study of Painting Techniques and Its Conservation State: Study of Painting Techniques and Its Conservation State. *J. Raman Spectrosc.* **2016**, *47*, 321–328. [CrossRef]
19. Cheilakou, E.; Troullinos, M.; Koui, M. Identification of Pigments on Byzantine Wall Paintings from Crete (14th Century AD) Using Non-Invasive Fiber Optics Diffuse Reflectance Spectroscopy (FORS). *J. Archaeol. Sci.* **2014**, *41*, 541–555. [CrossRef]
20. Cosentino, A. FORS Spectral Database of Historical Pigments in Different Binders. *E-Conser. J.* **2014**, *2*, 54–65. [CrossRef]
21. Corradini, M.; de Ferri, L.; Pojana, G. Fiber Optic Reflection Spectroscopy–Near-Infrared Characterization Study of Dry Pigments for Pictorial Retouching. *Appl. Spectrosc.* **2021**, *75*, 445–461. [CrossRef] [PubMed]
22. Piccolo, A.; Bonato, E.; Falchi, L.; Lucero-Gómez, P.; Barisoni, E.; Piccolo, M.; Balliana, E.; Cimino, D.; Izzo, F.C. A Comprehensive and Systematic Diagnostic Campaign for a New Acquisition of Contemporary Art—The Case of Natura Morta by Andreina Rosa (1924–2019) at the International Gallery of Modern Art Ca' Pesaro, Venice. *Heritage* **2021**, *4*, 4372–4398. [CrossRef]
23. Raicu, T.; Zollo, F.; Falchi, L.; Barisoni, E.; Piccolo, M.; Izzo, F.C. Preliminary Identification of Mixtures of Pigments Using the PaletteR Package in R—The Case of Six Paintings by Andreina Rosa (1924–2019) from the International Gallery of Modern Art Ca' Pesaro, Venice. *Heritage* **2023**, *6*, 524–547. [CrossRef]
24. Elias, M.; Chartier, C.; Prévot, G.; Garay, H.; Vignaud, C. The Colour of Ochres Explained by Their Composition. *Mater. Sci. Eng. B* **2006**, *127*, 70–80. [CrossRef]
25. Lorusso, S.; Natali, A.; Matteucci, C. Colorimetry Applied to the Field of Cultural Heritage: Examples of Study Cases. *Conserv. Sci. Cult. Herit.* **2007**, *7*, 187–220. [CrossRef]
26. Cavaleri, T.; Giovagnoli, A.; Nervo, M. Pigments and Mixtures Identification by Visible Reflectance Spectroscopy. *Procedia Chem.* **2013**, *8*, 45–54. [CrossRef]
27. Galli, A.; Caccia, M.; Bonizzoni, L.; Gargano, M.; Ludwig, N.; Poldi, G.; Martini, M. Deep inside the Color: How Optical Microscopy Contributes to the Elemental Characterization of a Painting. *Microchem. J.* **2020**, *155*, 104730. [CrossRef]
28. Lee, N.R.; Kim, S.J.; Moon, D.H. Non-Invasive Mineral Analysis of Pigments of Wall Paintings in the Sungseonjeon Hall. *Geosci. J.* **2022**, *27*, 161–176. [CrossRef]
29. Fioretti, G.; Clausi, M.; Eramo, G.; Longo, E.; Monno, A.; Pinto, D.; Tempesta, G. A Non-Invasive and Sustainable Characterization of Pigments in Wall Paintings: A Library of Apulian Colors. *Heritage* **2023**, *6*, 1567–1593. [CrossRef]
30. Folk, R.L. Bimodal supermature sandstones. Product of the desert floor. *XXIII Internat. Geol. Cong. Proc.* **1968**, *8*, 9–32.

31. McLAREN, K. XIII—The Development of the CIE 1976 (L* A* B*) Uniform Colour Space and Colour-difference Formula. *J. Soc. Dye. Colour.* **1976**, *92*, 338–341. [CrossRef]
32. Menges, F. Spectragryph—Optical Spectroscopy Software. 2022. Available online: http://www.effemm2.de/spectragryph/ (accessed on 10 February 2023).
33. Hradil, D.; Grygar, T.; Hradilová, J.; Bezdička, P. Clay and Iron Oxide Pigments in the History of Painting. *Appl. Clay Sci.* **2003**, *22*, 223–236. [CrossRef]
34. Mastrotheodoros, G.P.; Beltsios, K.G. Pigments—Iron-Based Red, Yellow, and Brown Ochres. *Archaeol. Anthropol. Sci.* **2022**, *14*, 35. [CrossRef]
35. Tomasini, E.; Siracusano, G.; Maier, M.S. Spectroscopic, Morphological and Chemical Characterization of Historic Pigments Based on Carbon. Paths for the Identification of an Artistic Pigment. *Microchem. J.* **2012**, *102*, 28–37. [CrossRef]
36. Kotulanová, E.; Bezdička, P.; Hradil, D.; Hradilová, J.; Švarcová, S.; Grygar, T. Degradation of Lead-Based Pigments by Salt Solutions. *J. Cult. Herit.* **2009**, *10*, 367–378. [CrossRef]
37. Švarcová, S.; Hradil, D.; Hradilová, J.; Čermáková, Z. Pigments—Copper-Based Greens and Blues. *Archaeol. Anthropol. Sci.* **2021**, *13*, 190. [CrossRef]
38. Konta, J. Clay and Man: Clay Raw Materials in the Service of Man. *Appl. Clay Sci.* **1995**, *10*, 275–335. [CrossRef]
39. Hofmann, C.; Rabitsch, S.; Malissa, A.; Aceto, M.; Uhlir, K.; Griesser, M.; Calà, E.; Agostino, A.; Fenoglio, G. The Miniatures of the Vienna Genesis: Colour Identification and Painters' Palettes. In *The Vienna Genesis*; Hofmann, C., Ed.; Böhlau Verlag: Wien, Austria, 2020; pp. 201–246. [CrossRef]
40. Villafana, T.; Edwards, G. Creation and Reference Characterization of Edo Period Japanese Woodblock Printing Ink Colorant Samples Using Multimodal Imaging and Reflectance Spectroscopy. *Herit. Sci.* **2019**, *7*, 94. [CrossRef]
41. Grazia, C.; Buti, D.; Amat, A.; Rosi, F.; Romani, A.; Domenici, D.; Sgamellotti, A.; Miliani, C. Shades of Blue: Non-Invasive Spectroscopic Investigations of Maya Blue Pigments. From Laboratory Mock-Ups to Mesoamerican Codices. *Herit. Sci.* **2020**, *8*, 1. [CrossRef]
42. Aceto, M. Pigments—The Palette of Organic Colourants in Wall Paintings. *Archaeol. Anthropol. Sci.* **2021**, *13*, 159. [CrossRef]
43. Brandi, C. *Teoria del Restauro, Rist*; Piccola Biblioteca Einaudi Arte, Teatro, Cinema, Musica; Giulio Einaudi: Torino, Italy, 2000.